Artificial saliva aerosol source and detection system for spreading analysis in indoor environments

Daniel Schiepel[1*], Robert Brinkema[1] and Daniel Schmeling[1]

[1] German Aerospace Center (DLR), Göttingen, Germany

[*]*Corresponding email: Daniel.Schiepel@DLR.de*

SUMMARY
In the context of the Corona pandemic the investigation of aerosol spreading is utmost important as the virus is transported within the aerosol particles exhaled by an infected person. Thus, a new aerosol generation and detection system is set up and employed in a ground-based research aircraft, a Dornier 728 located at DLR Göttingen, to investigate the large-scale aerosol-spreading. The system consists of an aerosol source generating a particle size distribution mimicking typical human exhalation with particles sizes between 0.3-2.5 µm and an array of Sensirion SPS30 particulate matter sensors. An accuracy assessment of the SPS30 sensors is conducted using a TSI OPS3330, a high-precision optical particle sizer. Low deviations of ±5 % of the particle concentration measured with the SPS30 with respect to the OPS are reported for concentrations below 2500/cm³ and +10% for particle densities up to 25'000/cm³. Within the Do728, the spreading distance with respect to a simulated infected passenger is within one row to the front and two to the back. Moreover, it is reported that the employment of heated passengers is crucial to simulate realistic aerosol spreading scenarios.

KEYWORDS
Aerosol generation, detection, spreading, aircraft cabin

INTRODUCTION
During the course of the Corona pandemic the investigation of the spreading routes of the SARS-CoV-2 virus has been one the of the main research tasks. It was found that the crucial route of the virus is its transportation within the aerosol particles exhaled by an infected person [1]. The concentration of exhaled aerosol particles of an infected person was investigated in [2] using influenza-infected test subjects. It is reported that they exhaled between 67 and 8,500 particles per liter of air with a geometric mean of 724 particles per liter.
Increasing concentrations of potentially virus-laden aerosol particles might become more problematic in enclosed environments like cars, rooms or aircraft. Focusing on the latter there are high air exchange rates and high-efficiency particulate air (HEPA) filters in place to reduce the level of aerosols (and other pollutants) in the air [3]. This simultaneously reduces the number of virus particles as they are transported within the aerosol particles from an infected passenger. The current state-of-the-art ventilation concept in passenger aircraft cabins is the so-called mixing ventilation [4]. Here, fresh air is supplied with high momentum from ceiling (CAO) and lateral air outlets (LAO) above and below the luggage compartments. This fresh (or filtered) air mixes with the heated used air from the passengers resulting in comfortable conditions. Simultaneously, a dilution and spreading of the potentially virus-laden aerosol particles occurs. Hence, it is unclear how far the particles will travel or how long it will take before they are removed from the cabin. However, the high degree of mixing also enhances the potential transport of aerosols from one passenger to another.
Addressing this transmission risk, costly in-flight experimental investigations were carried out [5]. For three selected aircraft types they estimated mean infection risks in the range from

1/1800 to 1/16 in case of super spreader. The aircraft were equipped with human puppets for in-flight measurements and during ground testing also heating blankets were used.
The quantification of this aerosol transport from a potentially infected passenger to the other passengers quantified in the present work using an aerosol-exhaling thermal manikin and a sensor system allowing for spatially resolved measurements of the aerosol concentration. Here, we validate the system and present its application within an aircraft cabin.

METHODS

Our approach for the acquisition of the aerosol spreading on larger scales is based on two components: One is a constant, stable and reliable aerosol exhalation and the other is an aerosol concentration acquisition system able to measure the concentrations at various places simultaneously.
We approach the spatially resolved measurement of particle number concentrations using Sensirion SPS30 particulate matter sensors. By default, the sensors return values of number concentrations binned for particle diameters ranges of 0.3-0.5 µm (PM0.5), 0.3-1 µm (PM1), 0.3-2.5 µm, (PM2.5) 0.3-4 µm (PM4) and 0.3-10 µm (PM10). From the datasheet it is known that only the ranges up to 2.5 µm are measured while the concentrations for the larger particle sizes >2.5 µm (PM4, PM10) are based on assumptions.

Figure 1: Photograph of the aerosol-exhaling facial mask connected to a thermal manikin. The exhaled aerosol particles are visualized by a laser light sheet.

The aerosol-exhalation is realized as an aerosol-exhaling facial mask with mouth and nose breathing capabilities. In Figure 1 a laser light sheet visualization of the exhalation process is presented revealing the aerosol cloud. To achieve this, three components are used: An aerosol generator, a pressurized air mixing system and a facial mask. The aerosol generator consists of an airbrush pistol (AFC-101A, nozzle diameter 0.35 mm) pressurized at 2 bars. It is used to disperse artificial saliva (mixed according to NRF 7.5 [6]) in a dispersion chamber. The generator is connected to a high-pressure air supply for mixing the aerosol particles with fresh air. Two high precision flow meters were used to measure the volume flow from the generator and from the fresh air allowing to control the volume flows separately using valves. Hence it is possible to adjust the aerosol particle concentration and volume flow for the outlet. A pipe system with an internally installed SPS30 sensor measures the aerosol concentration and connects to the facial mask. Combined with the volume flow at the outlet, this allows for a continuous monitoring of the aerosol generation rates.
The most important range for aerosol-based virus transmission is in the size range of 0.3-3 µm [7]. We validate our setup by a measurement of the particle concentration for different size bins using a high precision optical particle sizer (TSI OPS3330) after mixing the aerosols particles with the fresh air. The determined size distribution is presented in Figure 2 and a high particle

count for small particles (0.3 µm) can be reported which decreases for particles in the range of 0.4 µm. For particles around 1 µm an increasing particle concentration is reported which drops to virtually zero for particles beyond 2.5 µm. Thus, the generator achieves the desired spectrum and mimics typical human exhalation.
We designed the system with the application in cars, rooms and rolling stock in mind. Here, the air conditioning from the HVAC system reacts on the heat generated by the passenger. Thus, to trigger the appropriate working state we employ thermal manikins with a heat release of 75 W corresponding to the sensible heat release of a seated human. To simulate an infected passenger realistic conditions are provided by connecting our aerosol-exhaling facial mask to a thermal manikin giving it the appropriate thermal conditions in terms of thermal buoyancy and exhaust momentum.

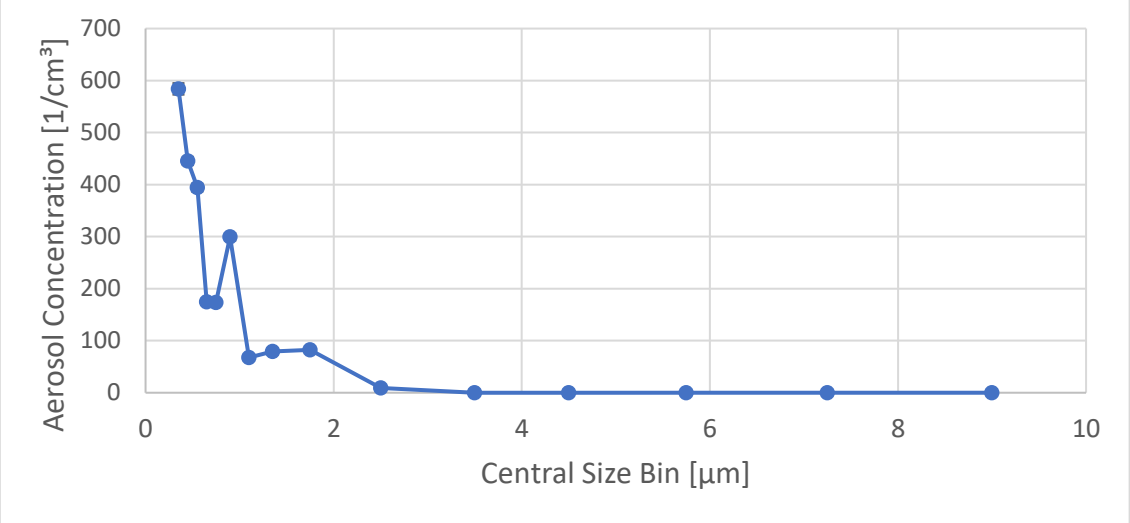

Figure 2: Particle concentration distribution depending on the particle size for the aerosol source measured with the OPS3330.

RESULTS AND DISCUSSION

The applicability of the SPS30 sensors to the generated aerosol is investigated by means of a comparison to the OPS3330. Therefore, a setup consisting of the aerosol source and a dilution system is used. A photograph of the setup is shown in Figure 3. The aerosol source is indicated by a) and the settling chamber by b). Typically, this would be connected to the facial mask but in this setup it is connected to a dilution stage with pressurized air supply to adjust the aerosol particle number concentration. The measurement stage is indicated by d) housing two SPS30 sensors and a connection for the OPS3330 (g)). As the range for the OPS is limited to below 3000 particles/cm³ two dilution stages can be employed f), with dilutions of 1:10 and 1:100 (or

Figure 3: Photograph of the SPS30 validation setup consisting primarily of the aerosol source a), a settling chamber b), a dilution stage c) and the measurement stage d) housing two SPS30 sensors and a connection for the OPS3330. The other shown parts are the notebooks for the data acquisition of the SPS and the OPS e), two dilution stages of the OPS f) and the OPS itself g).

combined 1:1000). Volume flow and aerosol concentrations are recorded using laptop computers e).

In Figure 4, the total measured particle number concentration for the bin range 0.3-2.5 µm acquired with the SPS30 sensors C_{SPS} is shown as a function of the OPS3330 readings C_{OPS}. In red, the total particle number concentration is presented. A clear dependency of both results is apparent: In general, the higher the particle concentration the higher both readings, yet the OPS detects higher particle concentrations compared to the SPS. The slope of the curve flattens for particle concentrations beyond 40'000/cm³.

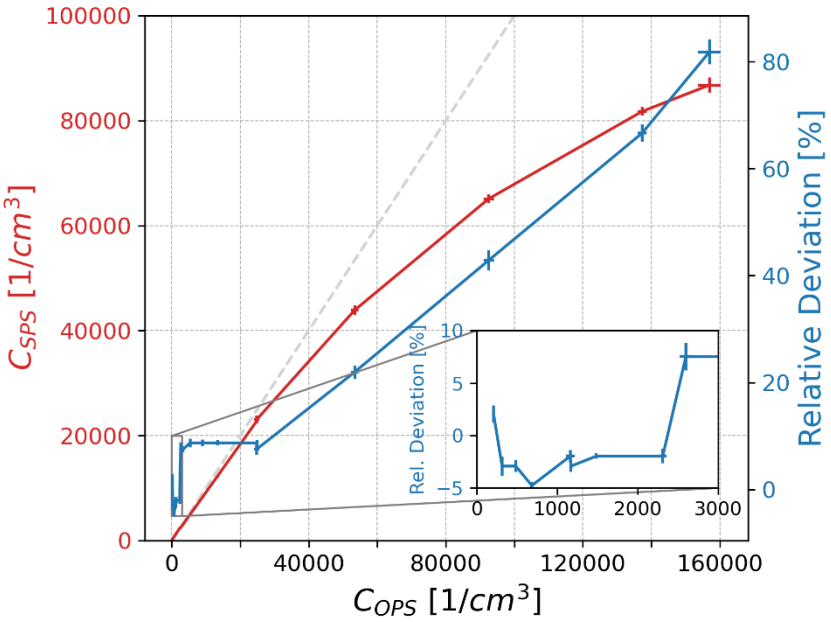

Figure 4: Calibration curve of the particle number concentration for the SPS30 sensors with respect to the OPS3330. In red the comparison of the absolute particle concentration and in blue the relative deviation. A close up view for low particle concentrations is presented in the lower right corner.

More insight on the dependency of the results is possible by evaluating the relative deviation $\frac{C_{OPS}}{C_{SPS}} - 1$. Using this definition, values larger than zero indicate a higher particle concentration measured with the OPS3330 compared to the SPS30 sensors and vice versa. This is presented Figure 4 as the blue curve for the entire concentration range with a zoomed version in the lower right corner. For low particle concentrations (<2500/cm³) a low relative deviation between ±5 % is reported. This increases to moderate deviations of +10% for particles concentrations above up to 25'000/cm³. Beyond, the deviation increases significantly. For the highest investigated particle concentration of 160'000/cm³ the optical particle sizer and the SPS30 sensor show a deviation of +80%. For typical particle number concentration occurring within a room for our aerosol source (<1000/cm³) this allows for spatially resolved measurements of the aerosol spreading using various of these low-cost sensors and even at concentrations of 25'000/cm³ the uncertainty increases only slightly.

An application example of the aerosol generation and detection system is given in the following. For more than 20 different scenarios the aerosol distribution within a 14 rows ground-based research aircraft (Dornier 728 [8]) is measured for state-of-the-art mixing ventilation (MV) on all 70 seats. No recirculating airflow is chosen which corresponds to 100% effective HEPA filters which is a good approximation of real-world efficiency of 99.97% [9]. Each seat is occupied with a thermal manikin featuring a SPS30 sensors in the breathing zone. The aerosol spreading is investigated by means of the aerosol-exhaling facial mask on one of the seats. Pre-tests revealed stable conditions after 10 to 15 minutes of aerosol exhalation. Based on these finding we defined the measurement scenarios as follows: First, the concerning case is set up. At t=0 s the aerosol exhalation is started and switched off after 20 minutes. The decay curves of the aerosol concentration are observed until background level is reached. An exemplary

aerosol concentration time series is presented in Figure 5 showing the aerosol concentration for the 0.3-2.5 µm bin. For the aerosol source located at seat E8, the concentration time series for three seats in different rows are shown. The concentrations reveal a similar behavior by starting at background level with particle concentrations close to zero at t=0 s and largely increasing values until around t=500 s stable conditions are reached. At t=1200 s the aerosol generator is turned off (indicated by the dashed red line) and the values decrease to background level which is reached at about t=1700 s. Yet, differences are found in the amplitudes and fluctuation for the three seats. While the seat in the row of the source (C8) reveals the highest values and fluctuations. Both are reduced for the seat two rows to the back (C10) and an even stronger suppression is reported for the seat two rows to the front (C6). The inlay on the right-hand side presents a close up view after turning off the aerosol source. Here, an exponential decay is apparent and a curve fitting to the data of seat C10 allowed to determine the decay constant $K = -1.60 \times 10^{-2}/s$. The resulting curve is indicated in dashed-light-blue. It is also found that the decay constant differs for the three seats. The influence on the fluctuations results from the strong turbulent mixing as close to the source the aerosol particles were not diluted opposed to the concentrations occurring at the seats further away. Moreover, based on the amplitudes of the aerosol concentrations it is reported that the aerosol particles tend to spread rather to the back than to the front. Differences in the decay constant indicated locally different removal efficiencies for the aerosol particles.

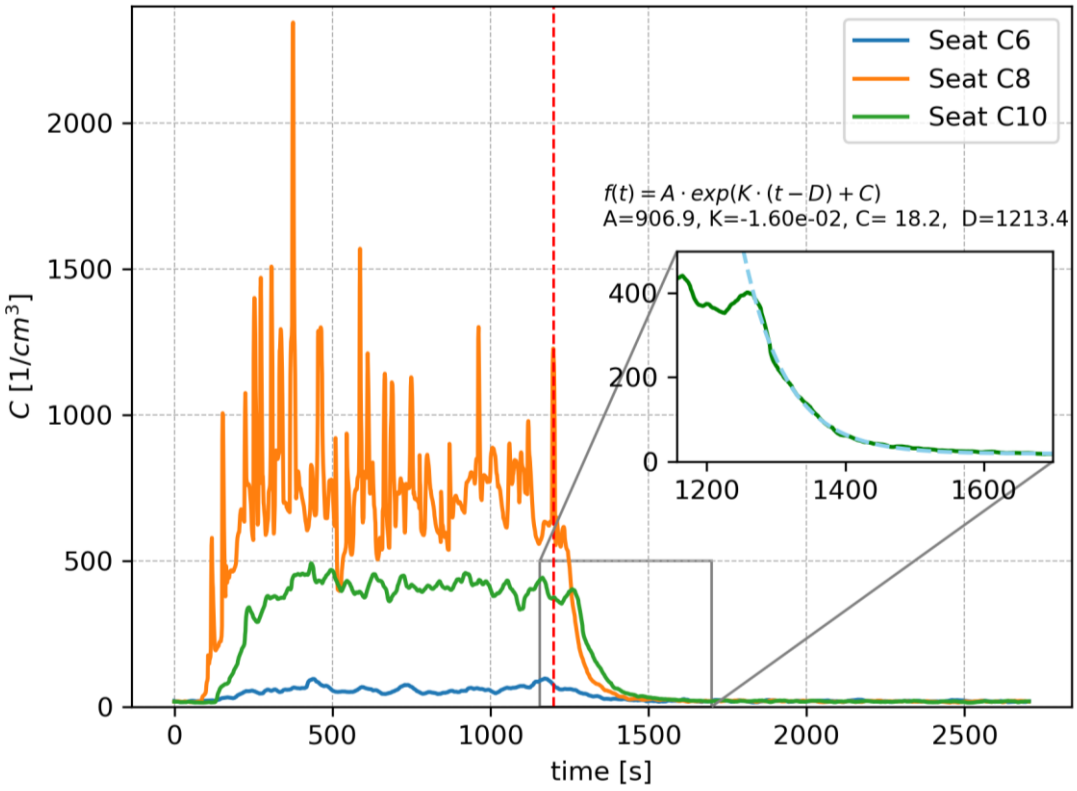

Figure 5: Aerosol concentration for the 0.3-2.5µm bin for three seats at different distances to the aerosol source.

A typical flight from Berlin to Helsinki takes T=1:55 h. Now, the most important question arising is the exposure to potentially virus-laden aerosol particles. The number of inhaled particles during this flight

$$N_{Flight} = \frac{C_{sick} \times \dot{V}_{Human}}{C_{,Source} \times \dot{V}_{Source}} \times C_{SPS} \times \dot{V}_{Human} \times T$$

can be determined by referencing the measured aerosol concentration C_{SPS} to the generated concentration C_{Source} with the accompanying volume flows $\dot{V}_{Human} = 6\,l/min$ and $\dot{V}_{Source} = 12\,l/min$. Finally, the typical exhaled aerosol particle concentration of a sick passenger C_{sick}=724/l [2] is used for scaling. The concentration values for C_{SPS} is determined as the mean value of the last 5 minutes prior to turning off the aerosol generator (dashed red

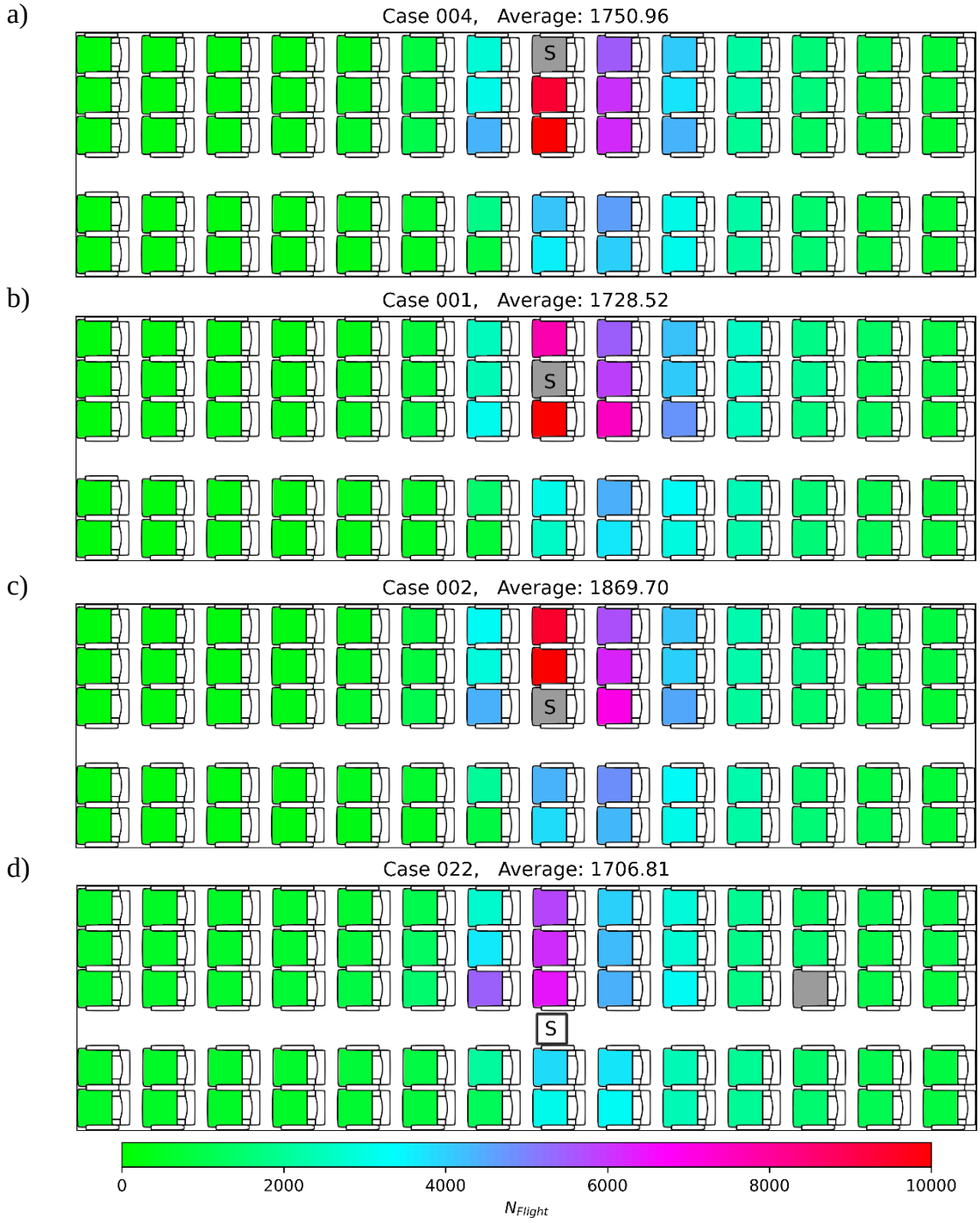

Figure 6: Aerosol distribution within the DO728 aircraft cabin for a source (S) wearing no mask for different seating positions (a-c) and while standing within the aisle (d).

line in Figure 5). As before, only the aerosol particles between 0.3 µm and 2.5 µm are considered for both, the source and the SPS30 sensors.

For a constant volume flow of 600 l/s of fresh air, 70 heated thermal manikins emitting heat at 75 W and an inlet temperature of 15°C, N_{Flight} during stationary conditions is investigated.

Figure 6 presents the distribution of N_{Flight} as a heat map projected onto the cross-section of the Do728 for the simulation of an infected passenger wearing no facial mask for different seating positions (a-c) and while standing within the aisle (d). In general, the spreading is well below 1500 inhaled particles for distances larger than one row to the front and two to the back from (S). The highest concentration values are found next to the source independent of the actual seat (a-c). The spreading across the aisle is largely suppressed by a factor of about three for all seated cases. Moreover, the window seat (a) reveals lower spreading to the back compared to (b) and (c). The simulation of an infected passenger standing in the aisle (d) results a different aerosol spreading map with an average particle number for smaller than for previous cases (a-c). This is a consequence of the downward airflow in the aisle area. Here, the air coming from the ceiling transports the aerosols to the floor and subsequently towards the exhaust openings. On top of each map, the average exposure considering all seats is presented. In general, the cases with seated passengers reveal higher average exposures compared to the standing source case. Still, especially the case with source in the aisle (c) reveals higher average concentrations (1870) compared to all other cases (1750/1729/1707).

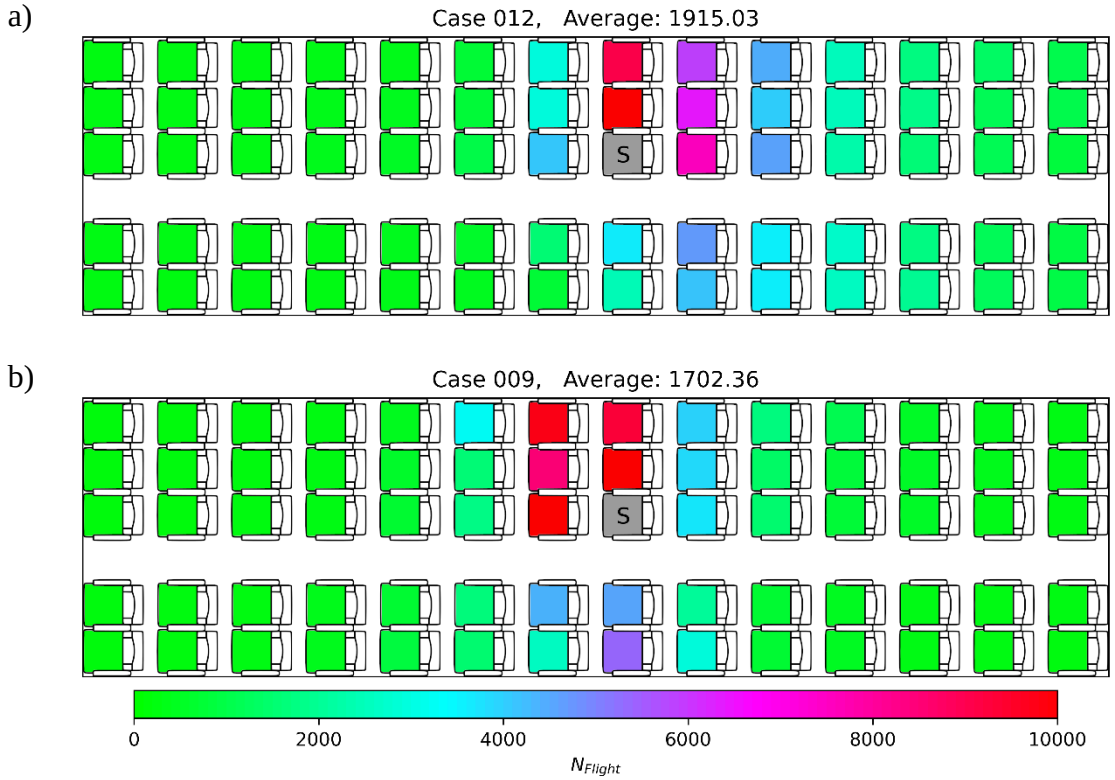

Figure 7: Aerosol distribution within the DO728 aircraft cabin for a source (S) wearing no mask for heated (a) and Non-heated (b) thermal manikins.

Addressing the question whether putting thermal loads into the cabin impacts the spreading of aerosol particles, we set up a testing case similar to the one before: A constant volume flow of 600 l/s of fresh air, an inlet temperature of 15°C and a potentially infected passenger wearing no mask. Here, we compared baseline case of the 70 thermal manikins emitting heat at 75 W to the one with manikins emitting no heat at all, i.e. all manikins are switched-off. The determined inhaled aerosol particle count N_{Flight} is presented in Figure 7. a) represents a reproducibility measurement of the reference case (Figure 6c) with heated manikins. The distribution looks virtually the same as before, an average deviation of only 2.4% is found, which confirms good repeatability by a low concerning the aerosol generation and spreading assessment. In Figure 7 b) for the non-heated case the inhaled particle distribution looks different compared to a). Now, the aerosol spreading to the rows in front of the source is significantly enhanced. Furthermore,

the spreading across the aisle has in increased even to the row in front of the source as compared to a). Taking these findings into account, it is concluded that simulating aircraft cabins with heat loads is of great importance to determine a realistic spreading of the aerosol particles.

CONCLUSION

In summary, a novel artificial saliva aerosol generation system with realistic human exhalation characteristics and particle diameters was presented. The system generates aerosol particle from artificial saliva with sizes between 0.3-2.5 µm. An accuracy assessment of the employed Sensirion SPS30 particulate matter sensors with respect to an optical particle sizer was conducted. Low deviations of ±5 % of the particle concentration measured with the SPS30 with respect to the OPS are reported for concentrations below 2500/cm³ and +10% for particle densities up to 25'000/cm³.

An aerosol spreading analysis using an array of SPS30 sensors allowed for spatially-resolved measurements in a ground-based research aircraft. By means of a simulated flight from Berlin to Helsinki the spreading distances for different scenarios were investigated. The spreading distance with respect to the simulated infected passenger is within one row to the front and two to the back. Moreover, it is reported that the employment of heated passengers is crucial to simulate realistic aerosol spreading scenarios.

The presented system can help virologists to estimate infection risks based on dose-response assumptions and typical travel durations. Moreover, the fundamental approach based on the dispersal analysis of pure artificial saliva guarantees the assignability to any other respiratory airborne contaminates and a quantitative measurement tool for the evaluation of aerodynamic counter measures to reduce airborne spreading in ventilated rooms and compartments.

REFERENCES

[1] (WHO), World Health Organization, "Coronavirus disease (covid-19): How is it transmitted?," 2022. [Online]. Available: https://www.who.int/news-room/questions-and-answers/item/coronavirus-disease-covid-19-how-is-it-transmitted. [Accessed 24 01 2022].

[2] P. Fabian, J. J. McDevitt, W. H. DeHaan, R. O. P. Fung, B. J. Cowling, K. H. Chan, G. M. Leung and D. K. Milton, "Influenza Virus in Human Exhaled Breath: An Observational Study," *PLoS ONE*, 16 7 2008.

[3] K. Bhuvan, R. Shrestha, P. Leggat, P. R. Shankar and S. Shrestha, "Safety of air travel during the ongoing COVID-19 pandemic," *Travel Med Infect Dis*, vol. 43, no. 102103, 2021.

[4] M. Kühn, J. Bosbach and C. Wagner, "Experimental parametric study of forced and mixed convection in a passenger aircraft cabin mock-up," *Building and Environment*, vol. 44, no. 5, pp. 961-970, 2009.

[5] Netherland Aerospace Center and National Institute for Public Health and the Environment, "Quantitative microbial risk assessment for aerosol transmission of SARS-CoV-2 in aircraft cabins based on measurement and simulations," NLR-CR-2021-232, 2021.

[6] B. D. Apothekerverbände, Deutscher Arzneimittel-Codex / Neues Rezeptur-Formularium, Eschborn: AVOXA - Mediengruppe Deutscher Apotheker GmbH, 2017.

[7] L. Morawska, *Indoor air, ventilation and infection transmission*, European Aerosol Conference, Online, 2021.

[8] J. Bosbach, S. Lange, G. Lauenroth, F. Hesselbach and M. Allzeit, "Alternative ventilation concepts for aircraft," *CEAS Aeronautical Journal*, vol. 4, p. 301–313, 2013.

[9] U.S. Environmental Protection Agency, "What is a HEPA filter?," 3 03 2021. [Online]. Available: https://www.epa.gov/indoor-air-quality-iaq/what-hepa-filter-1. [Accessed 26 01 2022].